Int. J. Heat Mass Transfer. Vol. 6, pp. 245–249. Pergamon Press 1963. Printed in Great Britain.

SHORTER COMMUNICATIONS

HEAT TRANSFER AND FRICTION IN TWO-DIMENSIONAL STAGNATION FLOW OF AIR WITH HELIUM INJECTION†

E. R. G. ECKERT, W. J. MINKOWYCZ, E. M. SPARROW and W. E. IBELE
Heat Transfer Laboratory, University of Minnesota, U.S.A.

(*Reviewed* 21 *October* 1962)

NOMENCLATURE

cf $= 2\tau_w/\rho_e u_e^2$, friction factor;
k, thermal conductivity;
$Nu_{x,e} = qx/(t_w - t_e)k_e$, Nusselt number;
q $= -k_w(\partial t/\partial y)_w$ heat flux per unit area and time at wall surface;
Re_x $= \rho u_e x/\mu$, Reynolds number ($Re_{x,e} = \rho_e u_e x/\mu_e$, $Re_x^* = \rho^* u_e x/\mu^*$);
t, absolute temperature;
u, v, velocity components in x- and y-direction;
w, helium mass fraction;
x, y, co-ordinates along and normal to wall surface;
ρ, density;
τ, shear stress.

Subscripts

e, outside boundary layer;
o, without helium injection;
w, at wall surface;
$*$, air properties based on reference temperature $(t_e + t_w)/2$.

PARALLELING an experimental program, an analysis was performed to obtain solutions for the heat transfer and flow characteristics of a two-dimensional stagnation-point flow in which air is the main stream gas and helium is injected into the boundary layer at the surface. The differential equations and boundary conditions describing the mass, momentum, and energy transport in such a boundary layer are contained in [1] and will not be repeated here. They are also identical with the boundary layer equations for flow along a surface with uniform pressure (flat plate) as given in the more easily accessible [2], with the exception that a pressure gradient term $\partial p/\partial x$ has to be added to the momentum equation and that the viscous dissipation term $\mu(\partial u/\partial y)^2$ has to be dropped from the energy equation. The partial differential equations were converted into total ones by a similarity transformation, and these then were put into the form of integral equations which were solved numerically on a Remington–Rand Univac 1103 electronic computer [2]. Properties of helium–air mixtures required for the computation were taken from [3]. Velocity, concentration, and temperature profiles as well as friction factors and heat-transfer coefficients were obtained in this way. The present note summarizes the results for the last two parameters.

Fig. 1 presents the ratio of the actual friction factor c_f to the friction factor c_{fo} for the same thermal boundary conditions, but with zero helium injection. This ratio is plotted against the helium mass fraction at the wall, w_w, for parametric values of the temperature t_e outside the boundary layer and of the ratio of wall temperature t_w to air temperature t_e. The friction factor c_{fo} itself can be obtained from Table 1.

Table 1

t_e (degR)	t_w/t_e	$\frac{1}{2}c_{fo}\sqrt{(Re_{x,e})}$
392	0·5	0·9717
540	1·2	1·314
1000	0·5	1·005
3000	0·25	0·8950
3000	0·50	1·014
5000	0·25	0·9118
5000	0·50	1·028

It is interesting to observe in Fig. 1 that the friction factor decreases only slightly with increasing helium mass fraction w_w or even increases for one set of boundary conditions. This is in contrast to the situation for a flat plate where the friction factor experiences a considerably larger decrease with blowing. The relative insensitivity of the stagnation-point results may be made plausible by recalling that the fluid within the boundary layer is subject to an accelerating pressure gradient. The effect of the pressure gradient will be greater when the density of the fluid in the boundary layer is relatively low compared with the density of the fluid in the main stream.

† These studies have been supported by the U.S. Air Force, Office of Scientific Research under Contract No. AF 49(638)-558.

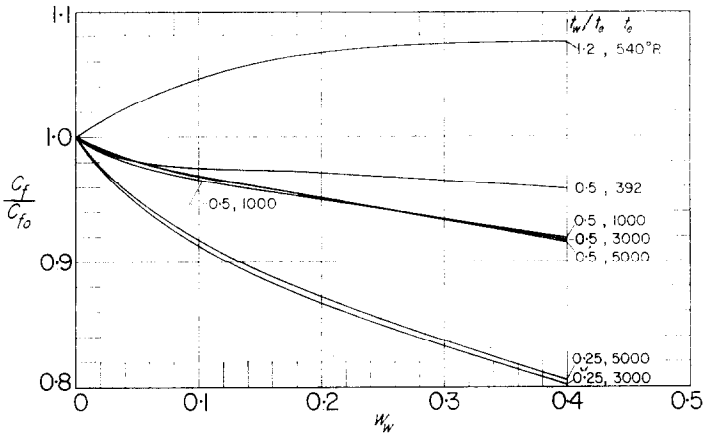

FIG. 1. Friction factor results.

The thus augmented acceleration tends to increase the wall shear, and therefore opposes the direct action of injection which tends to decrease the wall shear by blowing the boundary layer off the surface. For helium injection at the wall under conditions where $t_w/t_e \geqslant 1$, temperature and concentration work together to give a low fluid density near the wall. The effect of acceleration wins out and, as shown on the figure, the result is an increase in the friction factor. On the other hand, for a highly-cooled wall, the density increase due to low temperature tends to counteract the density decrease due to the presence of helium. The effect of the external pressure gradient is thus lessened and conditions become more comparable to those for a flat plate. This may be verified in the figure by noting that the greatest decrease in c_f occurs for the cases where the wall is most strongly cooled. The velocity profiles, which are not reproduced here, show for the same reason a considerable overshoot in the boundary layer over the value in the free stream, especially for the larger values of t_w/t_e.

Fig. 2 presents the heat-transfer parameter $Nu_{x,e}/\sqrt{(Re_{x,e})}$ plotted over the helium mass fraction w_w at the wall surface. It can be seen that the heat-transfer parameter decreases more strongly than the friction factor. An initial increase over the value for zero injection can be observed for some boundary conditions in the region of small injection rates. It is due to the fact that helium–air mixtures have a larger heat conductivity than does air alone. For the present analysis, as in [1] and [2], it was assumed that no air penetrates through the surface

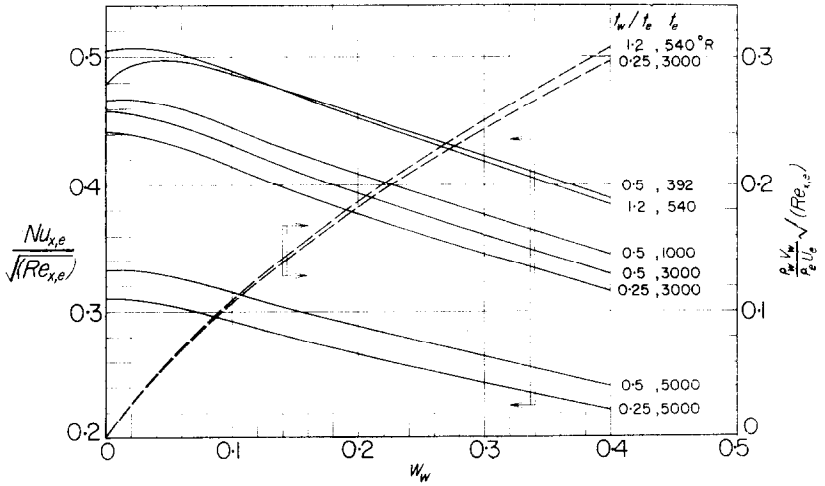

FIG. 2. Nusselt number results.

into the interior of the wall. Corresponding to this condition, there is a unique relationship between the wall mass fraction w_w and the injection parameter $\rho_w v_w / \rho_e u_e \sqrt{(Re_x, e)}$ which is a dimensionless representation of the helium mass release $\rho_w v_w$ at the wall surface per unit time and area. The dashed curves and the scale on the right-hand side of Fig. 2 present this relation for two pairs of boundary conditions. For the other boundary conditions covered in this analysis, the resulting curves are contained between the two shown in the figure.

Fig. 3, finally, presents the ratio of actual heat flux q at the wall surface to the heat flux at zero injection rate plotted over the injection parameter. In contrast to the previous figures, where properties were always introduced as they exist at the outer edge of the boundary layer, the properties in the injection parameter of Fig. 3 are based on a reference temperature as defined in the list of nomenclature. It should also be pointed out that the heat flux q defined in the same list includes only conductive transport from fluid to wall, and that the heat-transfer coefficient used for the calculation of the Nusselt number in Fig. 2 is based on this heat flux.

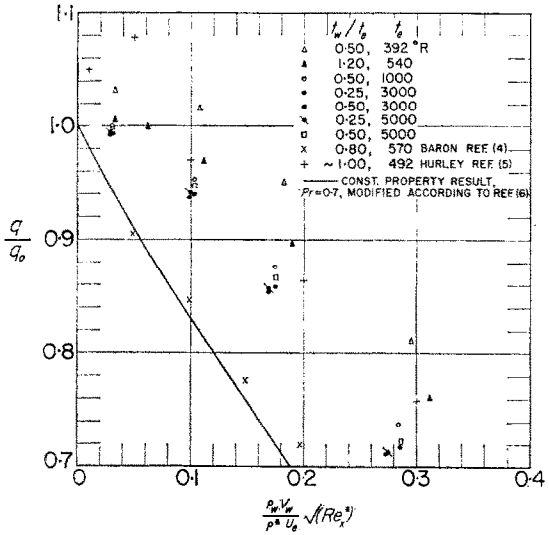

FIG. 3. Comparison of heat transfer with and without blowing.

Fig. 3 contains, in addition to the results of the present analysis, the results of two other investigations contained in the literature [4, 5]. The results of Hurley, indicated by upright crosses, are in their boundary condition fairly close to our analysis for $t_w/t_e = 1{\cdot}20$ and $t_e = 540°R$ The agreement between both results is good except for small values of the injection parameter, where Hurley obtained a larger overshoot of the heat flux ratio over the value 1 than did our analysis. In contrast, Baron's analysis resulted in considerably smaller heat flux ratios as indicated by the inclined crosses in Fig. 3. A detailed investigation and correspondence with Baron revealed that this difference is caused by the fact that Baron used in his analysis heat conductivity values as obtained from equation (B.22), [4]; whereas we used for our calculations heat conductivity values according to equations (1) and (2) in [3] because they are in closer agreement with experimental results. It appears, therefore, that the heat flux into the wall is quite sensitive to the values of the heat conductivity.

In [6], it was demonstrated that the friction factor ratio c_f/c_{f0} and the heat flux ratio q/q_0 as obtained by analyses for injection of different gases into laminar boundary layer flow of air over a flat plate can be expressed with good approximation as functions of a single parameter. This correlating parameter is formed by multiplying the injection parameter as used on the abscissa of Fig. 3 by the cube root of the ratio of the molecular weight of air to the molecular weight of the injected gas. It is also proposed in [6] to use the same procedure for the prediction of heat transfer and friction in stagnation-point flow. In order to check this procedure, a curve has been plotted in Fig. 3 which is obtained from Fig. 24 of [6] (or the larger scale Fig. 11 of [7]) by multiplying the abscissa values in that figure with the cube root of the ratio of the molecular weight of helium to the molecular weight of air. It may be observed that this curve represents the results of Baron's analysis fairly well, but does not agree with Hurley's and our own analysis. A further indication of the fact that the proposed procedure does not work generally is obtained from a study of Fig. 6 in [5]. In this figure, which presents the same heat-transfer parameter as used in our Fig. 2 plotted over the injection parameter, the water vapor results fall between that for hydrogen and helium, a situation which would not be predicted by the procedure of [6]. It appears that water vapor is an excellent coolant for mass transfer cooling of stagnation point flow.

The effects of thermal diffusion have not been included in the forementioned analyses. Some recent papers [8, 9] suggest that thermal diffusion can be important under certain conditions, for instance, when the differences between the wall temperature and main stream temperature are small. A research program, including analysis and experiments, whose aim is to clarify this effect, is now under preparation.

REFERENCES

1. A. A. HAYDAY, Mass transfer cooling in a laminar boundary layer in steady two-dimensional stagnation flow. Heat Transfer Laboratory, University of Minnesota, Tech. Note 19, (1958).
2. E. R. G. ECKERT, A. A. HAYDAY and W. J. MINKOWYCZ, Heat transfer, temperature recovery and skin friction on a flat plate with hydrogen release into a laminar boundary layer, *Int. J. Heat Mass Transfer*, **4**, 17–29 (1961).
3. E. R. G. ECKERT, W. E. IBELE and T. F. IRVINE JR, Prandtl number, thermal conductivity, and viscosity of air–helium mixtures. *NASA* TN D-533 (September 1960).
4. J. R. BARON and P. B. SCOTT, The laminar diffusion

boundary layer with external flow field pressure gradients. Massachusetts Institute of Technology, Naval Supersonic Laboratory, Tech. Rep. 419, (1959).
5. D. G. HURLEY, Mass transfer cooling in a boundary layer, *Aeronaut. Quart.* **XII**, 165–188 (1961).
6. J. F. GROSS, J. P. HARTNETT, D. J. MASSON and C. GAZLEY, JR, A review of binary laminar boundary layer characteristics, *Int. J. Heat Mass Transfer*, **3**, 198–221 (1961).
7. J. P. HARTNETT and E. R. G. ECKERT, Mass transfer cooling in a laminar boundary layer with constant fluid properties, *Trans. Amer. Soc. Mech. Engrs* **79**, 247–254 (1957).
8. J. R. BARON, Thermodynamic coupling in boundary layers. *J. Amer. Rocket Soc.* **32**, 1053–1059 (1962).
9. O. E. TEWFIK, E. R. G. ECKERT and C. J. SHIRTLIFFE, Thermal diffusion effects on energy transfer in a turbulent boundary layer. Proceedings, 1962 Heat Transfer and Fluid Mechanics Institute, Stanford University Press, 42–61 (1962).

TURBULENT HEAT TRANSFER IN A PARALLEL-PLATE CHANNEL

E. M. SPARROW and S. H. LIN
Heat Transfer Laboratory, University of Minnesota

(*Received* 3 *August* 1962)

THE purpose of this brief paper is to present analytical results for the fully developed heat-transfer characteristics of a turbulent flow in a parallel-plate channel with uniform wall heat flux. The results were obtained by integrating the energy equation utilizing a suitably chosen eddy diffusivity for heat. The analytical method parallels a prior study for the circular tube [1], and because of this, the details of the analysis will be omitted here. The circular tube results of [1] have received strong support from experiment (e.g. [2] and [3]). It is this good agreement which has prompted the present extension of the analysis to the parallel-plate channel. Friction factor results will also be given here.

The fully developed Nusselt numbers are presented in Fig. 1 as a function of Prandtl number for the range $Pr = 0{\cdot}7$ to 100. The Reynolds number, which appears as parameter, ranges from 10 000 to 500 000. The hydraulic diameter, D_e, is equal to twice the spacing between the plates; while the heat-transfer coefficient h is the ratio of the local heat flux to the local wall-to-bulk temperature difference. $\bar{U}$ is the mean velocity.

The results of the present analysis appear as solid lines on the figure. Also shown on the figure are dashed lines representing McAdams' [4] empirical correlation of circular tube data

$$Nu = 0{\cdot}023\ Re^{0{\cdot}8}\ Pr^{0{\cdot}4}. \qquad (1)$$

This correlation is usually regarded as applying as a first approximation to non-circular geometries provided that the hydraulic diameter is used. In addition, there are dot-dashed curves which represent the analytically-determined circular tube results of [1]; for $Re = 10^4$, only a single point was available and this is symbolized on the figure by a blackened circle. Finally, there is shown by triangles Deissler's [5] analytical findings for the parallel plate channel, available only for $Pr = 0{\cdot}73$. Aside from the latter, the authors are unaware of other analytical results for turbulent flow in a parallel-plate channel.

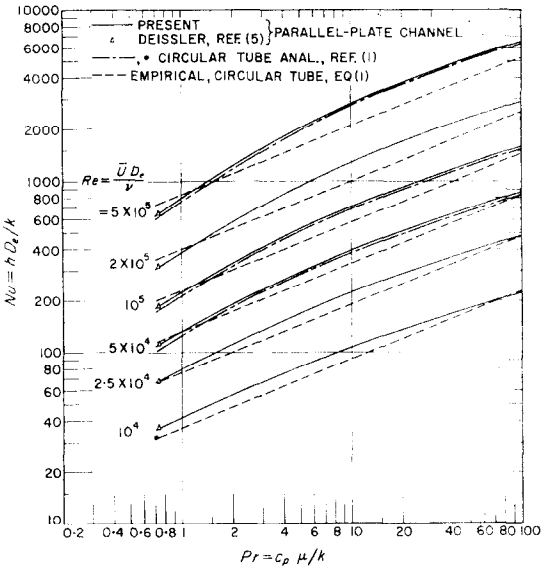

FIG. 1. Nusselt number results.

Comparison of the solid and dot-dashed curves indicates that the use of the hydraulic diameter is reasonably successful in bringing together the analytical results for the two geometries. Additionally, Deissler's results for $Pr = 0{\cdot}73$ are in good agreement with those of the present analysis.